5

Optimization of the Dynamic Behaviour of Complex Structures Based on a Multimodal Strategy

Sébastien Besset and Louis Jézéquel

École Centrale de Lyon
France

1. Introduction

The use of a modal approach to describe a structure from the standpoint of optimizing its dynamic behavior offers multiple advantages. Once modal matrices have been computed, optimization criteria can be readily defined. Both the dynamic amplification phenomena and dynamic coupling between substructures can then be described using just a small number of degrees of freedom. Furthermore, it becomes possible to link the criteria to the modal parameters used in the systemic procedure. In this chapter, we will propose optimization criteria based on a multimodal description of complex structures.

The modal synthesis technique presented herein is based on the double and triple-modal synthesis proposed by Besset & Jézéquel (2008a;d), as well as on classical component mode synthesis methods like those developed by Craig & Bampton (1968) or Hurty (1965). According to these modal synthesis techniques, many boundary degrees of freedom are capable of remaining; in such cases, numerical costs will also remain high. In order to avoid a high-cost situation, we are proposing generalized modal synthesis methods that operate by introducing generalized boundary coordinates in order to describe substructure connections: this procedure is called a "double modal synthesis".

In addition, we are proposing another procedure to analyze structures coupled with fluid. This second procedure will then be called "triple modal synthesis". The first modal synthesis is classical; it consists of representing the interior points of the fluid by acoustic modes. When considering a formulation in force, the pressure on boundary points is set equal to zero. Using a formulation in displacement, cavity modes are introduced, generating a correspondence to the free modes of a structure. The second modal synthesis consists of describing the boundary forces between the fluid and each substructure through use of a set of loaded modes. Lastly, the third modal synthesis consists of describing the boundary forces between each substructure by introducing another set of loaded modes.

Complex structures often include hollow parts and stiffeners, both of which require very accurate analysis in order to obtain satisfactory results. In this chapter, the term "hollow parts" will denote the formed steel and stiffeners that make up the skeleton of a structure. In complex structures such as automobiles, stiffeners and formed steel parts, which compose the skeleton of the structure, these parts are most responsible for overall structural behavior. To analyze these elements, the method used is the one proposed in Besset & Jezequel (2008b).

This study will focus on the acoustic parts of the coupled system using acoustic modes and based on a "triple modal synthesis method", which relies on a coupling formulation previously investigated by Morand & Ohayon (1995) and Ohayon (2001; 2003). An example of the modal analysis of a coupled system can be found in Sandberg et al. (2001). A modal analysis of the structure will yield modal mass and stiffness matrices, which can then be used to obtain effective modal parameters and in turn lead to criteria that allow optimizing the structure. These criteria will depend on the pressure values at points located in the acoustic parts of the system, e.g. inside a car, as a function of an excitation point located on a hollow part of the structure, e.g. a spar near the car engine. The criteria proposed herein allow for various vibrational propagation paths to be considered. It is thus possible to separately investigate the various noise sources within the structure.

The method proposed in this chapter may be used for any vibro-acoustic system. In fact, the ultimate goal of this approach is to define modal criteria that allow optimizing the vibro-acoustic system. Such criteria are related to the coupling terms between the systems' various substructures and are expressed as functions of the terms contained in the modal matrices. The number of criteria therefore depends on the number of substructures within the vibro-acoustic system. While our method will be described for the case of a specific system, keep in mind that it can be readily adapted to other vibro-acoustic systems.

The structure considered in this chapter is complex and comprises acoustic cavities, hollow parts and plates. The geometry of this structure is similar to that of a car. Two cavities will be considered. Consequently, this proposed method can be used to study all of the different paths through which vibrations propagate and generate noise within the car. Paths can exist through the hollow parts of the structure, as well as through the plates bounding the cavity and through the plates partitioning the two cavities.

2. Multimodal methodology

The purpose of the modal synthesis method is to describe a structure using several of its modes, most often the first modes. Many authors have already proposed such methods, based on either fixed or free interface modes. Among these authors, let's mention Hurty (1965) and Craig & Bampton (1968). This method consists of using fixed-interface modes and static deformations to describe each substructure constituting the studied system. Goldman (1968) and Hou (1969) proposed another method based on the structure's free modes.

One of the main advantages of modal synthesis is to provide a description of a structure using very few degrees of freedom, thus reducing numerical costs. This advantage is particularly useful when seeking to optimize structures involving many calculations. Although modal models can be developed through experimental testing, we focus herein on substructure models resulting from a finite element discretization.

Most structures can be divided into several substructures. After being analyzed, these substructures are most often assembled through boundary degrees of freedom. For example, Craig & Bampton (1968) proposed a method using both fixed-interface modes and constraint modes that correspond to the boundary degrees of freedom. Hence, many degrees of freedom may remain should the boundary size be large. To avoid this type of problem, Besset & Jézéquel (2008a;d) proposed a generalization of the modal synthesis method by introducing generalized boundary coordinates. This procedure is referred to as "double modal synthesis" or, if the system contains fluid parts, "triple modal synthesis". These two techniques will be described respectively in Sections 2.1 and 2.2.

2.1 Double modal synthesis method

The *double modal synthesis methode* has been proposed and described through a continuous formulation by Besset & Jézéquel (2008a). In this section, we will explain the role of the discretized formulation. In section 2.1.1, we will introduce a primal formulation based on the free modes of the structure. Section 2.1.2 will apply a dual formulation that uses fixed-interface modes. In both sections 2.1.1 and 2.1.2, both Figure 1 and the following notations and the following notations will be considered valid:

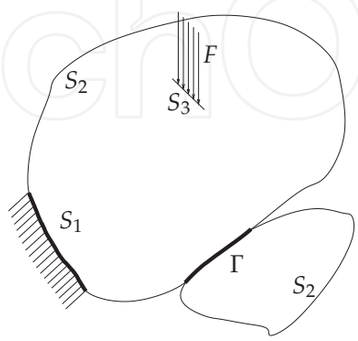

Fig. 1. Substructures and boundary conditions

- F is the force applied on the system;
- S_i are the boundaries of the system:
- Γ is the boundary between two substructures.

2.1.1 Primal formulation

The dynamic behaviour of the structure can be described through the following equation:

$$\left(-\omega^2 M + K\right) U = F \tag{1}$$

Considering the structure's free modes, U can be expressed as follows:

$$U = \phi_L q_L + \psi_r q_r + \psi_a q_a \tag{2}$$

where ϕ_L is the matrix of the structure's free modes, ψ_r the matrix of the n_r rigid body modes, and ψ_a is the attachment modes matrix associated with the free boundaries. ψ_a is obtained by imposing n_r boundary conditions, in order to suppress rigid body modes, while forces are applied on the free boundaries. If no rigid body modes are present, then ψ_a is the static flexibility matrix K^{-1}. If rigid body modes are present, then $\psi_a = A^T \psi_a^{\text{iso}} A$, where $A = I - M\psi_r M_{rr}^{-1} \psi_r^T$. ψ_a^{iso} is an isostatic flexibility matrix, obtained by imposing n_r boundary conditions on the structure and considering K_{iso}^{-1}. This method is intended to easily identify an isostatic flexibility matrix, which is corrected by adding rigid body modes, like for the finite element formulation of the Mac Neal method.
Equation 2 is then written considering the *double modal synthesis* theory, i.e. by expressing the boundary degrees of freedom as a fonction of k "branch modes" as follows:

$$U = \phi_L q_L + \psi_r q_r + \phi_b q_b \tag{3}$$

Matrix ϕ_b is the matrix of "branch modes", which are derived using the full structure equation condensed on interfaces. Let P be the matrix yielding generalized coordinates q_i as a function of displacements U (i.e. $U = P\{q_i\}$). Equation 1 then becomes:

$$\left[-\omega^2\left(P^T M P\right)+\left(P^T K P\right)\right]\left\{\begin{array}{c} q_L \\ q_r \\ q_b \end{array}\right\}=P^T F \tag{4}$$

2.1.2 Dual formulation

Like for the primal formulation described in section 2.1.1, the discretized equation of motion 1 is used herein:

$$\left(-\omega^2 M+K\right)U=F \tag{5}$$

In this section, U is expressed using fixed-interface modes:

$$U=\phi_F q_F+\psi_c q_c \tag{6}$$

As was the case for the discretization of the Craig and Bampton method Craig & Bampton (1968), matrices M and K are split into internal and boundary degrees of freedom, as follows:

$$U=\left\{\begin{array}{c} U_I \\ U_B \end{array}\right\},\quad M=\left[\begin{array}{cc} M_{II} & M_{IB} \\ M_{BI} & M_{BB} \end{array}\right],\quad K=\left[\begin{array}{cc} K_{II} & K_{IB} \\ K_{BI} & K_{BB} \end{array}\right] \tag{7}$$

The static flexibility can be written as K_{II}^{-1} and the constraint modes matrix is $\phi_c=K_{II}^{-1}K_{IB}$. The *double modal synthesis* theory is intended to express the remaining boundary degrees of freedom as a function of "branch modes" obtained by solving the following equation:

$$\left\{-\left[\omega^2\right]\left(P^T M P\right)+\left(P^T K P\right)\right\}\phi_D=0 \tag{8}$$

where $\left[\omega^2\right]$ is a diagonal matrix of eigenvalues corresponding to the columns of matrix ϕ_D. P is a transfer matrix that allows expressing U as a fuction of the generalized degrees of freedom q_F and q_c. Lastly, q_c can be expressed as $q_c=\phi_D q_b$ where q_b are the generalized boundary degrees of freedom.

2.2 Triple modal synthesis method

The *triple modal synthesis methode* has been proposed and described through a continuous formulation by Besset & Jézéquel (2008d). In this section, we will explain the discretized formulation. The structure and the notations used are recalled in figure 2.
We consider the discretized formulation of the coupled fluid-structure system, which leads to the following equations:

$$\left(-\omega^2 M+K\right)U=F \tag{9}$$

$$\left(-\omega^2 M_a+K_a\right)p=0 \tag{10}$$

Equation 9 pertains the structual part of the system, whereas Equation 10 relates to the acoustical part. This mixed formulation leads to the following equation:

$$\left(-\omega^2\underbrace{\left[\begin{array}{cc} M & 0 \\ C^T & M_a \end{array}\right]}_{\tilde{M}}+\underbrace{\left[\begin{array}{cc} K & -C \\ 0 & K_a \end{array}\right]}_{\tilde{K}}\right)\left\{\begin{array}{c} U \\ p \end{array}\right\}=\left\{\begin{array}{c} F \\ 0 \end{array}\right\} \tag{11}$$

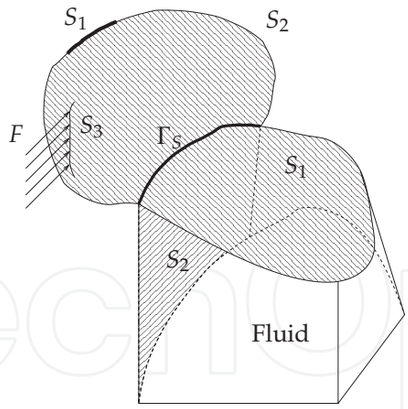

Fig. 2. Description of the triple modal synthesis

The *triple synthesis method* is performed by successively applying three modal syntheses. First, the behaviour of the fluid is expressed through "free modes" as follows:

$$p = \phi_p q_p \tag{12}$$

A second modal synthesis is then performed on the structural part of the system. Hence, the internal degrees of freedom, denoted U_i are expressed as follows:

$$U_i = \phi_i q_i + \psi_i u_j \tag{13}$$

where u_j are the boundary degrees of freedom. Lastly, a third modal synthesis is performed on the boundary degrees of freedom, i.e. degrees of freedom u_j are expressed as follows:

$$U_j = \phi_j q_j \tag{14}$$

Given Equations 12, 13 and 14, we can now define the following transfer matrix T:

$$\begin{Bmatrix} p \\ U_i \\ U_j \end{Bmatrix} = T \begin{Bmatrix} q_p \\ q_i \\ q_j \end{Bmatrix} \tag{15}$$

Equation 11 becomes:

$$\left[-\omega^2 \left(T^T \tilde{M} T\right) + \left(T^T \tilde{K} T\right)\right] \begin{Bmatrix} q_p \\ q_i \\ q_j \end{Bmatrix} = T^T F \tag{16}$$

3. Modal criteria and optimization

Optimization problems often lead to high calculation costs since the minimization function must be evaluated many times. The aim of this section is to propose modal-based criteria in order to optimize the dynamic behavior of complex structures. The examples provided herein will be applied on a schematic vehicle geometry 3. The structural case will be analyzed first in Section 3.1. Optimization criteria are linked to the "vibration paths" between substructures. The fluid-structure coupling case will then be presented in Section 3.2.

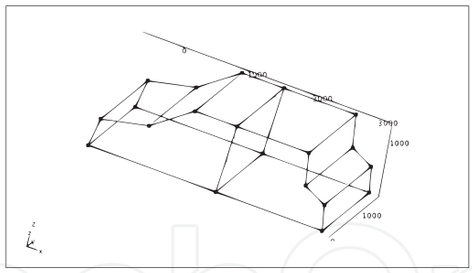

Fig. 3. Structure to be optimized

3.1 Criteria based on double modal synthesis method

This section presents the optimization criteria based on the double modal synthesis method derived in Section 2.1. These criteria are close to the modal matrices used for the modal synthesis of the structure. Once the structure has been analyzed, it therefore becomes very straightforward to calculate the optimization criteria. We will begin by explaining how to derive the modal-based criteria and indicating their use in the optimization step. Afterwards, we will demonstrate the efficiency of these parameters by optimizing the structure shown in Figure 3.

3.1.1 Modal-based criteria

The criteria proposed in this section are based on modal parameters that link degrees of freedom subjected to a displacement (so-called excited degrees of freedom) with the degrees of freedom whose displacements are to be minimized. In order to obtain these modal parameters, we will apply the double modal synthesis method proposed in Section 2.1. However, we will proceed by separating the degrees of freedom that will be excited; these degrees of freedom will remain nodal.

Let's now introduce the following notations concerning the degrees of freedom of the structure:

- u_P are the degrees of freedom relative to the plates;
- u_{Hb} are the degrees of freedom relative to the boundaries between plates.

The excitations will be relevant to the some degrees of freedom we have denoted u_{Hb}. These degrees of freedom will be denoted u_{He}. The double modal synthesis theory then leads to the expression in Equation 17:

$$\begin{cases} u_P = \Phi_P q_P + \Psi_P u_{Hb} + \Psi_{Pe} u_{He} \\ u_{Hb} = \Phi_{Hb} q_{Hb} \end{cases} \tag{17}$$

Thanks to the orthogonal properties of the modes used in the modal analysis, the motion equation can now be written as follows, in considering the damping matrix that we have assumed to be diagonal:

$$\left(-\omega^2 \begin{bmatrix} M_{EE} & M_{EHb} & M_{EP} \\ M_{HbE} & m_{Hbk} & M_{HbP} \\ M_{PE} & M_{PHb} & m_{Pk} \end{bmatrix} + i\omega \begin{bmatrix} 0 & 0 & 0 \\ 0 & c_{Hbk} & 0 \\ 0 & 0 & c_{Pk} \end{bmatrix} + \begin{bmatrix} K_{EE} & K_{EHb} & 0 \\ K_{HbE} & k_{Hbk} & 0 \\ 0 & 0 & k_{Pk} \end{bmatrix} \right) \begin{Bmatrix} u_{He} \\ q_{Hb} \\ q_P \end{Bmatrix} = \begin{Bmatrix} \overline{f}_E \\ \overline{f}_{Hb} \\ \overline{f}_P \end{Bmatrix} \tag{18}$$

where matrices $[m_{Hbk}]$, $[m_{Pk}]$, $[k_{Hbk}]$, $[k_{Pk}]$, $[c_{Hbk}]$, $[c_{Pk}]$ and $[c_{Hck}]$ are diagonal matrices.
To obtain the modal parameters, u_P must be expressed as a function of f_P and u_{He}. Let's express one of the last rows in equation 34:

$$-\omega^2\left(M_{PE}^k u_{He} + M_{PHb}^k q_{Hb} + m_{Pk} q_P^k\right) + i\omega c_{Pk} q_P^k + k_{Pk} q_P^k = \overline{f}_P^k \tag{19}$$

M_{PE}^k, M_{PHb}^k are the k^{th} rows of matrices M_{PE}, M_{PHb}. $\overline{f}_P$ can be expressed as a function of f_P as follow:

$$\overline{f}_P = \Phi_P^T f_P \tag{20}$$

Equation 19 then becomes:

$$q_P^k = \frac{\Phi_P^{kT} f_P + \omega^2\left(M_{PE}^k u_{He} + M_{PHb}^k q_{Hb}\right)}{-\omega^2 m_{Pk} + i\omega c_{Pk} + k_{Pk}} \tag{21}$$

where Φ_P^k is the k^{th} column of Φ_P. Equation 21 can now be written as:

$$\begin{aligned} u_P &= \sum_k \Phi_P^k q_{Pk} + \Psi_P u_{Hb} + \Psi_{Pe} u_{He} \\ &= \sum_k \left(\frac{\Phi_P^k \Phi_P^{kT}}{-\omega^2 m_{Pk} + i\omega c_{Pk} + k_{Pk}}\right) f_P \\ &\quad + \left[\sum_k \left(\frac{\omega^2 \Phi_P^k M_{PE}^k}{-\omega^2 m_{Pk} + i\omega c_{Pk} + k_{Pk}}\right) + \Psi_{Pe}\right] u_{He} \\ &\quad + \left[\sum_k \left(\frac{\omega^2 \Phi_P^k \tilde{M}_{PHb}^k}{-\omega^2 m_{Pk} + i\omega c_{Pk} + k_{Pk}}\right) + \Psi_P\right] u_{Hb} \end{aligned} \tag{22}$$

where $M_{PHb}^k = \tilde{M}_{PHb}^k \Phi_{Hb}$.
Two modal parameters can be deduced from Equation 22. First, the dynamic flexibility matrix G is given by:

$$G(\omega) = \sum_k \left(\frac{\Phi_P^k \Phi_P^{kT}}{-\omega^2 m_{Pk} + i\omega c_{Pk} + k_{Pk}}\right) \tag{23}$$

This first parameter corresponds to the relation between a force applied on a plate and the displacements it generates.
Secondly, by ignoring the static terms corresponding to the boundaries, the transmissibility matrix T is given by:

$$T(\omega) = \sum_k \left(\frac{\omega^2 \Phi_P^k M_{PE}^k}{-\omega^2 m_{Pk} + i\omega c_{Pk} + k_{Pk}}\right) \tag{24}$$

This equation corresponds to the relation between excitation and the displacements it generates on the plate. Note that this excitation is a displacement excitation. This expression can be rewritten using parameters $\tilde{G}$ and $\tilde{T}$ as follows:

$$G(\omega) = \sum_k \frac{1}{1 - \left(\frac{\omega}{\omega_k}\right)^2 + 2i\xi_k \frac{\omega}{\omega_k}} \tilde{G}_k \tag{25}$$

$$T(\omega) = \sum_k \frac{\left(\frac{\omega}{\omega_k}\right)^2}{1 - \left(\frac{\omega}{\omega_k}\right)^2 + 2i\xi_k \frac{\omega}{\omega_k}} \tilde{T}_k \tag{26}$$

where

$$\tilde{G}_k = \frac{\Phi_P^k \Phi_P^{kT}}{\omega_k^2 m_{Pk}} \tag{27}$$

$$\tilde{T}_k = \frac{\Phi_P^k M_{PE}^k}{m_{Pk}} \tag{28}$$

with the notations $c_{Pk} = 2\xi_k \sqrt{k_{Pk} m_{Pk}}$ and $\omega_k = \sqrt{\frac{k_{Pk}}{m_{Pk}}}$. Matrices $\tilde{G}_k$ and $\tilde{T}_k$ are referred to as modal parameters.

3.1.2 Example of optimization using modal parameters

In this section, we will deduce criteria from the flexibility and transmissibility matrices proposed in section 3.1.1. The sums $\sum_k ()$ appearing in these matrices correspond to a mode superposition. The optimization criteria can thus be written as follows:

$$C_G = \max_k \left| \frac{\Phi_P^k \Phi_P^{kT}}{\omega_k^2 m_{Pk}} \right| \tag{29}$$

$$C_T = \max_k \left| \frac{\Phi_P^k M_{PE}^k}{m_{Pk}} \right| \tag{30}$$

where the norm $|x|$ is the maximum component of matrix x. In considering these criteria, it is possible to optimize the structure. Moreover, obtaining the value $k_{\max}$ informs which mode is responsible for the value of the criteria.

The method proposed in this section has been tested on a complex structure that includes hollow parts and plates. The parameters we have chosen to optimize are correlated with the geometry of the hollow parts. We will in fact be optimizing D and λ, as shown in figure 4.

The optimization methods used in the next sections will introduce both D and λ as parameters. The hollow parts of the structure shown in figure 8 are split into 8 parts, and each part is optimized with optimal values of D and λ. Thus, 16 parameters are to be optimized.

The analysis of criteria C_G and C_T indicates which modes are responsible for the displacements that need to be reduced. Figure 6 shows the values of C_G^k, which are part of the criterion C_G:

$$C_G^k = \left| \frac{\Phi_P^k \Phi_P^{kT}}{\omega_k^2 m_{Pk}} \right| \tag{31}$$

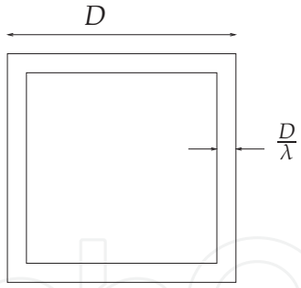

Fig. 4. Hollow part included in the structure

The same analysis can now be conducted for C_T^k:

$$C_T^k = \left| \frac{\Phi_P^k M_{PE}^k}{m_{Pk}} \right| \tag{32}$$

Figure 5 displays the values of C_T^k, which are part of the criterion C_T.

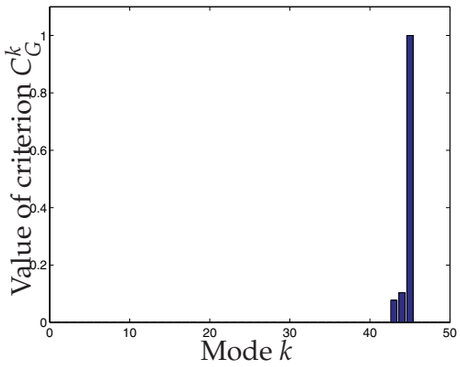

Fig. 5. Values of C_G^k

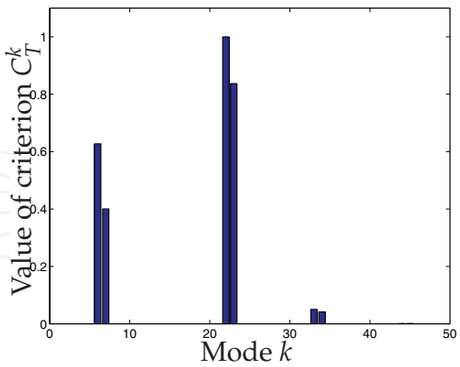

Fig. 6. Values of C_T^k

Figures 5 and 6 reveal that criteria C_G and C_T do not necessarily depend on the same modes. In this example, we only analyze the criteria for the first 50 modes of the structure. Figure 5 shows that the 45$^{\text{th}}$ mode is mainly responsible for the value of criterion C_G, whereas Figure 6 suggests that the 6$^{\text{th}}$, 7$^{\text{th}}$, 22$^{\text{th}}$ and 23$^{\text{th}}$ modes are responsible for the value of criterion C_T. It is therefore necessary to take these two criteria into account in order to optimize the structure.

In this section, we will present the results obtained using a classical genetic algorithm. Figure 7 shows the Pareto diagram of the sets (λ_i, D_i). The units on x and y axes are not important since they depend on the values of c_g and c_t.

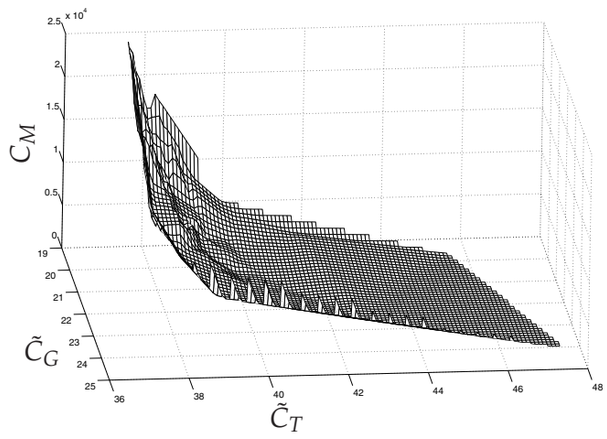

Fig. 7. Pareto points

3.2 Criteria based on triple modal synthesis method

In this section, we will condider the acoustical part inside the structure. The criteria presented here are similar to those from section 3.1, although they take into account this fluid part.

3.2.1 Modal-based criteria

The structure considered herein is complex and includes hollow parts and plates. It has been built using formed steel, which makes up its skeleton (as presented in Figure 8). The plates are fixed to this skeleton and form two cavities inside the structure (see the figure). Like in Section 3.1, the structure's geometry is similar to that of a car, for the purpose of highlighting that the proposed methods can be applied to an industrial context.

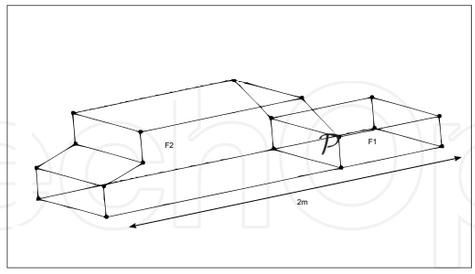

Fig. 8. The structure to be optimized

Figure 8 shows the geometry of the vibro-acoustic system under consideration. It is composed of plates and two fluid cavities. The degrees of freedom denoted u_{P_1} correspond to the plates, with the exception of the plates denoted $\mathcal{P}$ in figure 8, the degrees of freedom denoted u_{P_2} correspond to plate $\mathcal{P}$ in figure 8. Moreover, the degrees of freedom denoted p_{F_1} (resp. p_{F_2}) correspond to the pressure in the first cavity, as labeled $\mathcal{F}_1$ in figure 8 (resp. the second cavity, $\mathcal{F}_2$ in figure 8). The approach adopted in this section to study the vibro-acoustic behavior is a (u, p) formulation. Like in Section3.1.1, generalized degrees of freedom are correlated with nodal degrees of freedom through the following equations:

$$\begin{cases} u_{Hb} = \Phi_{Hb} q_{Hb} \\ u_{P_1} = \Phi_{P1} q_{P1} + \Psi_{P1} u_{Hb} + \Psi_{P1e} u_E \\ u_{P_2} = \Phi_{P2} q_{P2} + \Psi_{P2} u_{Hb} + \Psi_{P2e} u_E \\ p_{F_1} = \Phi_{F1} q_{F1} \\ p_{F_2} = \Phi_{F2} q_{F2} \end{cases} \tag{33}$$

According to the *triple modal synthesis* theory, as explained in section 2.2, the motion equation can be written as follows:

$$\left(-\omega^2 \begin{bmatrix} \overline{M}_{EE} & \overline{M}_{EHc} & 0 & \overline{M}_{EP1} & \overline{M}_{EP2} & 0 & 0 \\ \overline{M}_{HcE} & m_{Hc} & \overline{M}_{HcHb} & 0 & 0 & 0 & 0 \\ 0 & \overline{M}_{HbHc} & m_{Hb} & \overline{M}_{HbP1} & \overline{M}_{HbP2} & 0 & 0 \\ \overline{M}_{P1E} & 0 & \overline{M}_{P1Hb} & m_{P1} & 0 & 0 & 0 \\ \overline{M}_{P2E} & 0 & \overline{M}_{P2Hb} & 0 & m_{P2} & 0 & 0 \\ \overline{M}_{F1E} & 0 & \overline{M}_{F1Hb} & \overline{M}_{F1P1} & \overline{M}_{F1P2} & m_{F1} & 0 \\ \overline{M}_{F2E} & 0 & \overline{M}_{F2Hb} & \overline{M}_{F2P1} & \overline{M}_{F2P2} & 0 & m_{F2} \end{bmatrix} \right.$$

$$+ i\omega \begin{bmatrix} 0 & 0 & 0 & 0 & 0 & 0 & 0 \\ 0 & c_{Hc} & 0 & 0 & 0 & 0 & 0 \\ 0 & 0 & c_{Hb} & 0 & 0 & 0 & 0 \\ 0 & 0 & 0 & c_{P1} & 0 & 0 & 0 \\ 0 & 0 & 0 & 0 & c_{P2} & 0 & 0 \\ 0 & 0 & 0 & 0 & 0 & c_{F1} & 0 \\ 0 & 0 & 0 & 0 & 0 & 0 & c_{F2} \end{bmatrix}$$

$$\left. + \begin{bmatrix} \overline{K}_{EE} & 0 & 0 & 0 & 0 & \overline{K}_{EF1} & \overline{K}_{EF2} \\ 0 & k_{Hc} & 0 & 0 & 0 & \overline{K}_{HcF1} & \overline{K}_{HcF2} \\ 0 & 0 & k_{Hb} & 0 & 0 & \overline{K}_{HbF1} & \overline{K}_{HbF2} \\ 0 & 0 & 0 & k_{P1} & 0 & \overline{K}_{P1F1} & \overline{K}_{P1F2} \\ 0 & 0 & 0 & 0 & k_{P2} & \overline{K}_{P2F1} & \overline{K}_{P2F2} \\ 0 & 0 & 0 & 0 & 0 & k_{F1} & 0 \\ 0 & 0 & 0 & 0 & 0 & 0 & k_{F2} \end{bmatrix} \right) \begin{Bmatrix} u_E \\ q_{Hc} \\ q_{Hb} \\ q_{P1} \\ q_{P2} \\ q_{F1} \\ q_{F2} \end{Bmatrix} = \begin{Bmatrix} \overline{f}_E \\ \overline{f}_{Hc} \\ \overline{f}_{Hb} \\ \overline{f}_{P1} \\ \overline{f}_{P2} \\ 0 \\ 0 \end{Bmatrix} \tag{34}$$

The purpose of this section is to express the pressure p_{F_2} in the second cavity as a function of the structural displacements. This expression will allow the various vibrational paths to be distinguished from one another. The problem must be studied using a systemic approach. Certain criteria related to the various vibrational paths will thus be defined. Using the last row of Equation 34, the following expression is obtained:

$$-\omega^2 \left(\overline{M}^k_{F2E} u_E + \overline{M}^k_{F2Hb} q_{Hb} + \overline{M}^k_{F2P1} q_{P1} + \overline{M}^k_{F2P2} q_{P2} + m^k_{F2} q^k_{F2} \right) + i\omega c^k_{F2} q^k_{F2} + k^k_{F2} q^k_{F2} = 0 \tag{35}$$

where $\overline{M}^k_{F2E}$, $\overline{M}^k_{F2Hb}$, $\overline{M}^k_{F2P1}$ and $\overline{M}^k_{F2P2}$ are the k^{th} rows of matrices $\overline{M}_{F2E}$, $\overline{M}_{F2Hc}$, $\overline{M}_{F2Hb}$, $\overline{M}_{F2P1}$ and $\overline{M}_{F2P2}$. q^k_{F2} is the k^{th} component of vector q_{F2}.
Equation 35 leads to:

$$q_{F2}^k = \frac{\omega^2 \left(\overline{M}_{F2E}^k u_E + \overline{M}_{F2Hb}^k q_{Hb} + \overline{M}_{F2P1}^k q_{P1} + \overline{M}_{F2P2}^k q_{P2} \right)}{-\omega^2 m_{F2}^k + i\omega c_{F2}^k + k_{F2}^k} \tag{36}$$

Now let Φ_{F2}^k be the k^{th} column of Φ_{F2}. Combining Equations 33 and 36 yields:

$$\begin{aligned} p_{F_2} &= \sum_k \Phi_{F2}^k q_{F2}^k \\ &= \sum_k \left[\frac{\omega^2 \Phi_{F2}^k \overline{M}_{F2E}^k}{-\omega^2 m_{F2}^k + i\omega c_{F2}^k + k_{F2}^k} \right] u_E \\ &\quad + \sum_k \left[\frac{\omega^2 \Phi_{F2}^k \overline{M}_{F2Hb}^k}{-\omega^2 m_{F2}^k + i\omega c_{F2}^k + k_{F2}^k} \right] \tilde{\Phi}_{Hb} u_{Hb} \\ &\quad + \sum_k \left[\frac{\omega^2 \Phi_{F2}^k \overline{M}_{F2P1}^k}{-\omega^2 m_{F2}^k + i\omega c_{F2}^k + k_{F2}^k} \right] \left(\tilde{\Phi}_{P1} \left(u_{P1} - \Psi_{P1} u_{Hb} - \Psi_{P1e} u_E \right) \right) \\ &\quad + \sum_k \left[\frac{\omega^2 \Phi_{F2}^k \overline{M}_{F2P2}^k}{-\omega^2 m_{F2}^k + i\omega c_{F2}^k + k_{F2}^k} \right] \left(\tilde{\Phi}_{P2} \left(u_{P2} - \Psi_{P2} u_{Hb} - \Psi_{P2e} u_E \right) \right) \end{aligned} \tag{37}$$

The quantities with a "tilde" are left pseudo-inverse matrices. It is possible to define several pseudo-inverse matrices. In the case of singular systems, pseudo-inverse matrices enable finding solutions (c.f. Farhat & Géradin (1998)). In the present case, the matrices are not square and the solution obtained is a least squares approximation, due to the fact that modal synthesis does not entail fewer modes than the number of physical degrees of freedom for the system.

Equation 37 provides an approximation to the pressure field p_{F_2} in the second cavity as a function of structural displacements. A superposition of the substructural modes clearly appears in the sums $\sum_k (\,)$.

Equation 37 allows for the definition of modal parameters, which can then be used to optimize the coupled system. These parameters correspond to each of the various vibrational paths, i.e.: a direct path, a path through the hollow parts of the structure, a path through the plates bounding the cavity, and a path through the plate located between the two cavities.

3.2.1.1 Direct path

The direct path is directly obtained via Equation 37, it corresponds to an excitation point on a plate located next to cavity $\mathcal{F}_2$. Let's recall that the excitations considered herein are displacement excitations.

The modal parameter corresponding to this direct path is denoted $G_E(\omega)$:

$$G_E(\omega) = \sum_k \frac{\left(\frac{\omega}{\omega_k}\right)^2}{1 - \left(\frac{\omega}{\omega_k}\right)^2 + 2i\xi_k \frac{\omega}{\omega_k}} \tilde{G}_E^k \tag{38}$$

where:

$$\tilde{G}_E^k = \frac{\Phi_{F2}^k \left(\overline{M}_{F2E}^k - \overline{M}_{F2P1}^k \tilde{\Phi}_{P1} \Psi_{P1e} - \overline{M}_{F2P2}^k \tilde{\Phi}_{P2} \Psi_{P2e} \right)}{m_{P2}^k} \tag{39}$$

with the notations $c_{F2}^k = 2\xi_k \sqrt{k_{F2}^k m_{F2}^k}$ and $\omega_k = \sqrt{\frac{k_{F2}^k}{m_{F2}^k}}$.

3.2.1.2 Path through the boundaries

The path through the boundaries is given by component u_{Hb} of Equation 37.
q_{Hb}^k can now be expressed according to the third row of Equation 34:

$$\begin{aligned} -\omega^2 \left(\overline{M}_{HbHc}^k q_{Hc} + m_{Hb}^k q_{Hb}^k + \overline{M}_{HbP1}^k q_{P1} + \overline{M}_{HbP2}^k q_{P2} \right) \\ + i\omega c_{Hb}^k q_{Hb}^k + k_{Hb}^k q_{Hb}^k + \overline{K}_{HbF1}^k q_{F1} + \overline{K}_{HbF2}^k q_{F2} = \overline{f}_{Hb}^k \end{aligned} \tag{40}$$

The modal parameter corresponding to the path through the hollow parts is denoted $G_H(\omega)$. Using Equations 40 and 35 together, it is possible to write:

$$G_H(\omega) = \left(\sum_k \frac{\left(\frac{\omega}{\omega_{1k}}\right)^2}{1 - \left(\frac{\omega}{\omega_{1k}}\right)^2 + 2i\xi_{1k}\frac{\omega}{\omega_{1k}}} \tilde{G}_{H1}^k \right) \left(\sum_k \frac{\left(\frac{\omega}{\omega_{2k}}\right)^2}{1 - \left(\frac{\omega}{\omega_{2k}}\right)^2 + 2i\xi_{2k}\frac{\omega}{\omega_{2k}}} \tilde{G}_{H2}^k \right) \tag{41}$$

where:

$$\tilde{G}_{H1}^k = \frac{\Phi_{F2}^k \overline{M}_{F2Hb}^k \tilde{\Phi}_{Hb}}{m_{F2}^k} \tag{42}$$

$$\tilde{G}_{H2}^k = \frac{\Phi_{Hb}^k \left(\overline{M}_{HbHc}^k \tilde{\Phi}_{Hc} \Psi_{He} - \overline{M}_{HbP1}^k \tilde{\Phi}_{P1} \Psi_{P1e} - \overline{M}_{HbP2}^k \tilde{\Phi}_{P2} \Psi_{P2e} \right)}{m_{Hb}^k} \tag{43}$$

with the notations $c_{F2}^k = 2\xi_{1k}\sqrt{k_{F2}^k m_{F2}^k}$, $\omega_{1k} = \sqrt{\frac{k_{F2}^k}{m_{F2}^k}}$, and $c_{Hb}^k = 2\xi_{2k}\sqrt{k_{Hb}^k m_{Hb}^k}$ and $\omega_{2k} = \sqrt{\frac{k_{Hb}^k}{m_{Hb}^k}}$.

3.2.1.3 Path through the plates

The path through the plates is given by component u_{P1} of Equation 37.
u_{P1} can then be written as a function of u_E according to the fourth row of Equation 34:

$$\begin{aligned} -\omega^2 \left(\overline{M}_{P1E}^k u_E + \overline{M}_{P1Hb}^k q_{Hb} + m_{P1}^k q_{P1}^k \right) \\ + i\omega c_{P1}^k q_{P1}^k + k_{P1}^k q_{P1}^k + \overline{K}_{P1F1} q_{F1} + \overline{K}_{P1F2} q_{F2} = \overline{f}_{P1} \end{aligned} \tag{44}$$

The modal parameter corresponding to the path through the plates is denoted $G_{P1}(\omega)$. By combining Equations 44 and 35, it is now possible to write:

$$G^1_{P1}(\omega) = \left(\sum_k \frac{\left(\frac{\omega}{\omega_{1k}}\right)^2}{1 - \left(\frac{\omega}{\omega_{1k}}\right)^2 + 2i\xi_{1k}\frac{\omega}{\omega_{1k}}} \tilde{G}^k_{P11} \right) \left(\sum_k \frac{\left(\frac{\omega}{\omega_{2k}}\right)^2}{1 - \left(\frac{\omega}{\omega_{2k}}\right)^2 + 2i\xi_{2k}\frac{\omega}{\omega_{2k}}} \tilde{G}^k_{P12} \right) \tag{45}$$

$$\begin{aligned} G^2_{P1}(\omega) = & \left(\sum_k \frac{\left(\frac{\omega}{\omega_{1k}}\right)^2}{1 - \left(\frac{\omega}{\omega_{1k}}\right)^2 + 2i\xi_{1k}\frac{\omega}{\omega_{1k}}} \tilde{G}^k_{P11} \right) \\ & \times \left(\sum_k \frac{\left(\frac{\omega}{\omega_{2k}}\right)^2}{1 - \left(\frac{\omega}{\omega_{2k}}\right)^2 + 2i\xi_{2k}\frac{\omega}{\omega_{2k}}} \tilde{G}^k_{P13} \right) \\ & \times \left(\sum_k \frac{\left(\frac{\omega}{\omega_{3k}}\right)^2}{1 - \left(\frac{\omega}{\omega_{3k}}\right)^2 + 2i\xi_{3k}\frac{\omega}{\omega_{3k}}} \tilde{G}^k_{P14} \right) \end{aligned} \tag{46}$$

where:

$$\tilde{G}^k_{P11} = \frac{\Phi^k_{F2}\overline{M}^k_{F2P1}\tilde{\Phi}_{P1}}{m^k_{F2}} \tag{47}$$

$$\tilde{G}^k_{P12} = \frac{\Phi^k_{P1}\overline{M}^k_{P1E}}{m^k_{P1}} \tag{48}$$

$$\tilde{G}^k_{P13} = \frac{\Phi^k_{P1}\overline{M}^k_{P1Hb}\tilde{\Phi}_{Hb}}{m^k_{P1}} \tag{49}$$

$$\tilde{G}^k_{P14} = \tilde{G}^k_{H2} \quad \text{(see Equation 43)} \tag{50}$$

with the notations $c^k_{F2} = 2\xi_{1k}\sqrt{k^k_{F2}m^k_{F2}}$, $\omega_{1k} = \sqrt{\frac{k^k_{F2}}{m^k_{F2}}}$, $c^k_{P1} = 2\xi_{2k}\sqrt{k^k_{P1}m^k_{P1}}$, $\omega_{2k} = \sqrt{\frac{k^k_{P1}}{m^k_{P1}}}$, $c^k_{Hb} = 2\xi_{3k}\sqrt{k^k_{Hb}m^k_{Hb}}$ and $\omega_{3k} = \sqrt{\frac{k^k_{Hb}}{m^k_{Hb}}}$.

3.2.1.4 Path through the first cavity

The path through the first cavity is related to the plate forming the boundary between the two cavities.

The modal parameter corresponding to this path can be written according to the fifth and sixth rows of Equation 34:

$$-\omega^2\left(\overline{M}^k_{P2E}u_E+\overline{M}^k_{P2Hb}q_{Hb}+m^k_{P2}q^k_{P2}\right)+i\omega c^k_{P2}q^k_{P2}+k^k_{P2}q^k_{P2}+\overline{K}^k_{P2F1}q_{F1}+\overline{K}^k_{P2F2}q_{F2}=\overline{f}_{P2} \quad (51)$$

$$-\omega^2\left(\overline{M}^k_{F1E}u_E+\overline{M}^k_{F1Hb}q_{Hb}+\overline{M}^k_{F1P1}q_{P1}+\overline{M}^k_{F1P2}q^k_{P2}+m^k_{F1}q_{F1}\right)+i\omega c^k_{F1}q^k_{F1}+k^k_{F1}q^k_{F1}=0 \quad (52)$$

The modal parameter corresponding to the path through the plates is denoted $G_{P2}(\omega)$. By combining Equations 51, 52 and 35, it becomes possible to write:

$$G_{P2}(\omega)=\left(\sum_k\frac{\left(\frac{\omega}{\omega_{1k}}\right)^2}{1-\left(\frac{\omega}{\omega_{1k}}\right)^2+2i\xi_{1k}\frac{\omega}{\omega_{1k}}}\tilde{G}^k_{P21}\right)\times\left(\sum_k\frac{1}{1-\left(\frac{\omega}{\omega_{2k}}\right)^2+2i\xi_{2k}\frac{\omega}{\omega_{2k}}}\tilde{G}^k_{P22}\right)\times\left(\sum_k\frac{\left(\frac{\omega}{\omega_{3k}}\right)^2}{1-\left(\frac{\omega}{\omega_{3k}}\right)^2+2i\xi_{3k}\frac{\omega}{\omega_{3k}}}\tilde{G}^k_{P23}\right) \quad (53)$$

where:

$$\tilde{G}^k_{P21}=\frac{\Phi^k_{F2}\overline{M}^k_{F2P2}\tilde{\Phi}_{P2}}{m^k_{F2}} \quad (54)$$

$$\tilde{G}^k_{P22}=\frac{\Phi^k_{P2}\overline{K}^k_{P2F1}\tilde{\Phi}_{F1}}{\omega^2_{2k}m^k_{P2}} \quad (55)$$

$$\tilde{G}^k_{P23}=\frac{\Phi^k_{F1}\left(\overline{M}^k_{F1E}-\overline{M}^k_{F1P1}\tilde{\Phi}_{P1}\Psi_{P1e}-\overline{M}^k_{F1P2}\tilde{\Phi}_{P2}\Psi_{P2e}\right)}{m^k_{F1}} \quad (56)$$

with the notations $c^k_{F2}=2\xi_{1k}\sqrt{k^k_{F2}m^k_{F2}}$, $\omega_{1k}=\sqrt{\frac{k^k_{F2}}{m^k_{F2}}}$, $c^k_{P2}=2\xi_{2k}\sqrt{k^k_{P2}m^k_{P2}}$, $\omega_{2k}=\sqrt{\frac{k^k_{P2}}{m^k_{P2}}}$, $c^k_{F1}=2\xi_{3k}\sqrt{k^k_{F1}m^k_{F1}}$ and $\omega_{3k}=\sqrt{\frac{k^k_{F1}}{m^k_{F1}}}$.

3.2.1.5 Modal criteria

The modal parameters defined in the previous sections now lead to the criteria defined as follows:

$$C_E = \max_k \left| \frac{\left(\frac{\omega}{\omega_k}\right)^2}{1 - \left(\frac{\omega}{\omega_k}\right)^2 + 2i\xi_k \frac{\omega}{\omega_k}} \tilde{G}_E^k \right| \tag{57}$$

$$C_n = \max_k \left| \frac{\left(\frac{\omega}{\omega_{1k}}\right)^2}{1 - \left(\frac{\omega}{\omega_{1k}}\right)^2 + 2i\xi_{1k} \frac{\omega}{\omega_{1k}}} \tilde{G}_n^k \right| \quad \text{where } n \text{ can be } H1,\ P11 \text{ or } P21 \tag{58}$$

$$C_n = \max_k \left| \frac{\left(\frac{\omega}{\omega_{2k}}\right)^2}{1 - \left(\frac{\omega}{\omega_{2k}}\right)^2 + 2i\xi_{2k} \frac{\omega}{\omega_{2k}}} \tilde{G}_n^k \right| \quad \text{where } n \text{ can be } H2,\ P12, \text{ or } P13 \tag{59}$$

$$C_{P14} = \max_k \left| \frac{\left(\frac{\omega}{\omega_{3k}}\right)^2}{1 - \left(\frac{\omega}{\omega_{3k}}\right)^2 + 2i\xi_{3k} \frac{\omega}{\omega_{3k}}} \tilde{G}_{P14}^k \right| \tag{60}$$

$$C_{P22} = \max_k \left| \frac{1}{1 - \left(\frac{\omega}{\omega_{2k}}\right)^2 + 2i\xi_{2k} \frac{\omega}{\omega_{2k}}} \tilde{G}_{P22}^k \right| \tag{61}$$

$$C_{P23} = \max_k \left| \frac{\left(\frac{\omega}{\omega_{3k}}\right)^2}{1 - \left(\frac{\omega}{\omega_{3k}}\right)^2 + 2i\xi_{3k} \frac{\omega}{\omega_{3k}}} \tilde{G}_{P23}^k \right| \tag{62}$$

Within the framework of an optimization problem, it is possible to use these criteria, for example, in order to optimize a structural geometry. However, the criteria we are proposing do not allow for derivation with respect to any of the structural parameters (e.g. geometry of the hollow parts, plate thickness…), although many optimization methods require derivatives of these criteria. For this reason, other criteria related to the original set of criteria will be defined in the next section.

As indicated below, criteria C_n (where n can be E, $H1$, $H2$, $P11$, $P12$, $P13$, $P14$, $P21$, $P22$ or $P23$) cannot be derived with respect to any parameter, even though this would be useful in most optimization problems. To remedy this shortcoming, we introduce criteria $\tilde{C}_n$, defined as follows:

$$\tilde{C}_n = \frac{1}{4} \log \sum_k \left| \lambda(\omega, k)\, \tilde{G}_n^k \right|^4 \tag{63}$$

where $\lambda(\omega)$ is a coefficient that depends on ω. This is the case, for example, of $\tilde{G}_E^k$, $\lambda(\omega) = \frac{\left(\frac{\omega}{\omega_k}\right)^2}{1 - \left(\frac{\omega}{\omega_k}\right)^2 + 2i\xi_k \frac{\omega}{\omega_k}}$.

It has been demonstrated that these criteria are very similar to the first set and have nearly the same minima and maxima Besset & Jézéquel (2008c).

3.2.2 Analysis of the criteria

In this section, the criteria developed in the previous sections will be analyzed. In order to simplify the analysis, only one excitation point placed on a hollow part bounding the first cavity $\mathcal{F}_1$ is considered.

The values of criteria C_n may change with the excitation frequency due to the coefficient $\lambda(\omega)$. It can be observed that the strength of each criterion depends on the excitation frequency. For example, it is interesting to note that criterion $CP22$ increases more strongly than the other criteria with frequency f. Therefore, the vibrational path through plate $\mathcal{P}$ becomes very significant at higher frequencies.

NLet's also note that criteria $CP13$ and $CH2$ show peaks that correspond to the global modes of the structure, since the modal matrices of the structure's hollow parts are involved in these criteria.

Modal parameters $\tilde{G}^k_{H1}$, $\tilde{G}^k_{H2}$, $\tilde{G}^k_{P21}$, $\tilde{G}^k_{P22}$, $\tilde{G}^k_{P23}$, $\tilde{G}^k_{P11}$, $\tilde{G}^k_{P13}$ and $\tilde{G}^k_{P14}$ have all been analyzed. This step will allow each of the modes responsible for the values of criteria C_n to be defined. The modal parameters must be weighted with the previously defined coefficients $\lambda(\omega)$, in order to take the excitation frequency into account. Two cases of excitation are presented, i.e. at 50 Hz and at 300 Hz.

3.2.2.1 Path through the first cavity

Considering the vibrational path through the first cavity and plate $\mathcal{P}$, three modal parameters need to be analyzed. Figures 9, 10 and 11 display the values of modal parameters $\tilde{G}^k_{P21}$, $\tilde{G}^k_{P22}$ and $\tilde{G}^k_{P23}$ as a function of the mode number k, for an excitation frequency of 50 Hz. Figures 12, 13 and 14 show these same parameters for an excitation frequency of 300 Hz.

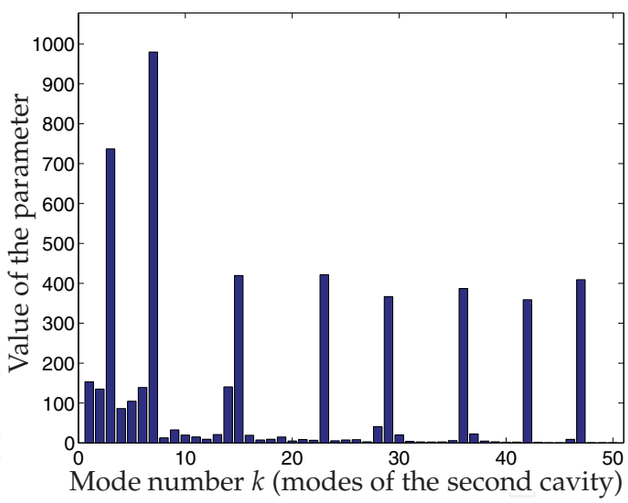

Fig. 9. Values of parameter $\left|\lambda \tilde{G}^k_{P21}\right|$ as a function of k – 50 Hz

Figure 10 shows that only one mode of plate $\mathcal{P}$ is responsible for the transmission of vibrations between the first and second cavities. The criterion associated with this figure is C_{P22}, which is related to the influence of pressure in the first cavity on plate $\mathcal{P}$. Given that the action of an acoustic fluid on a structure is not very significant when compared with that of a structure on a fluid, the parameter values given in figure 10 remain very small. For an influence to be exerted on the path through the first cavity, which is the objective of this section, one could, for example, restrict the influence of the mode presented in figure 10.

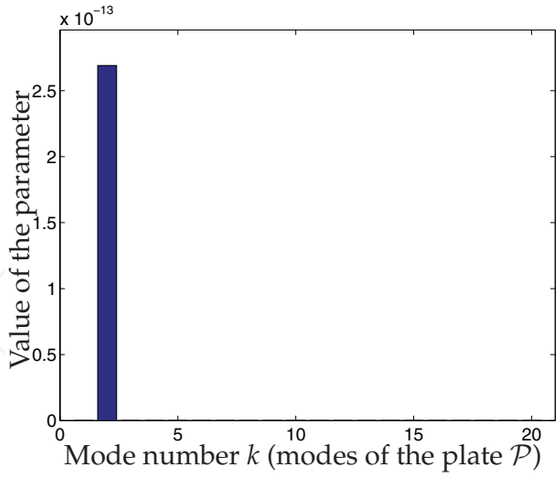

Fig. 10. Values of parameter $\left|\lambda \tilde{G}^{k}_{P22}\right|$ as a function of k – 50 Hz

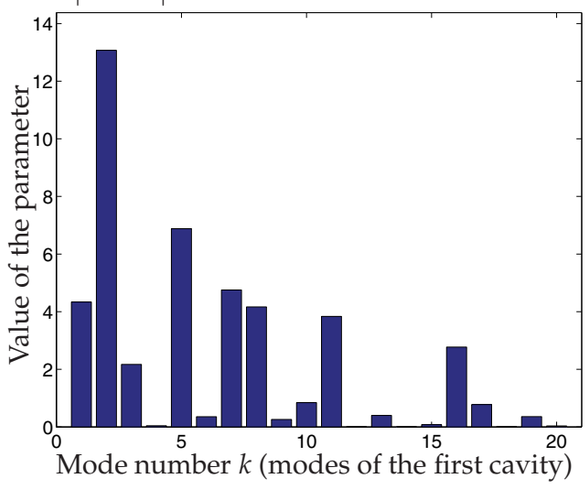

Fig. 11. Values of parameter $\left|\lambda \tilde{G}^{k}_{P23}\right|$ as a function of k – 50 Hz

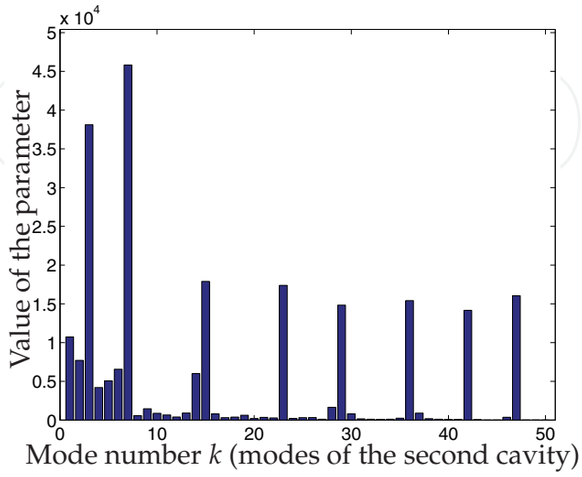

Fig. 12. Values of parameter $\left|\lambda \tilde{G}^{k}_{P21}\right|$ as a function of k – 300 Hz

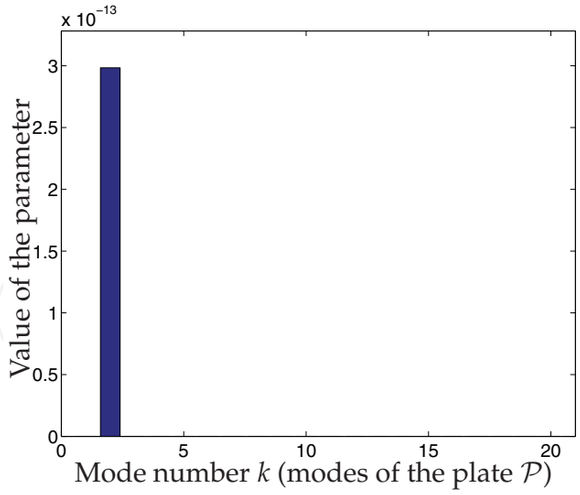

Fig. 13. Values of parameter $\left|\lambda \tilde{G}^k_{P22}\right|$ as a function of k – 300 Hz

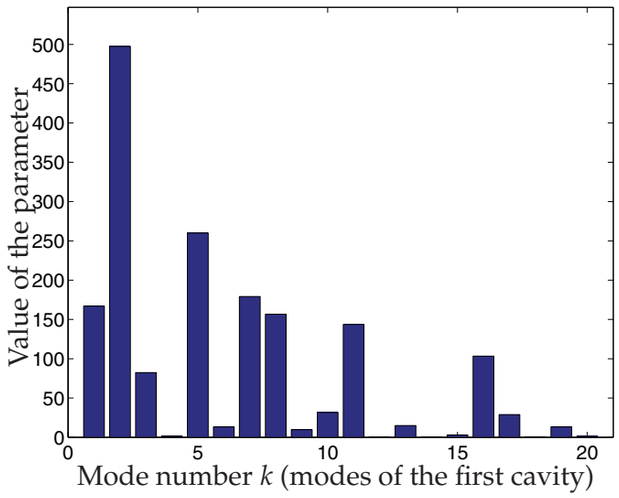

Fig. 14. Values of parameter $\left|\lambda \tilde{G}^k_{P23}\right|$ as a function of k – 300 Hz

3.2.2.2 Path through the hollow parts

For the vibrational path through the hollow parts, two modal parameters need to be analyzed. Figures 15 and 16 show the values of modal parameters $\tilde{G}^k_{H1}$ and $\tilde{G}^k_{H2}$ as a function of mode number k for an excitation frequency of 50 Hz. Figures 15 and 16 show these same parameters for an excitation frequency of 300 Hz.

In figures 15 and 16, it can be seen that many of the modes are strong. The values of these parameters increase with excitation frequency. However, the values for criterion C_{H2} are much smaller than those for criterion C_{H1}. It then becomes possible to elect to optimize the structure using C_{H1}, which seems to exert a stronger influence on the transmission of vibrations. Although the influence of criterion C_{H2} appears to be smaller, the use of this criterion in structural optimization allows studying the vibrational path through the plates, as described in the following section.

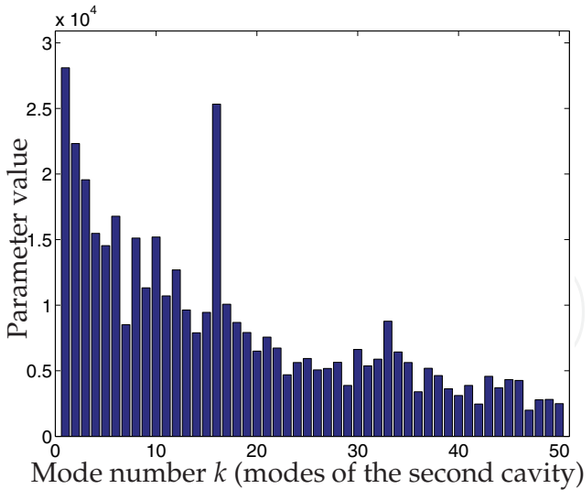

Fig. 15. Values of parameter $\left|\lambda \tilde{G}^k_{H1}\right|$ as a function of k – 50 Hz

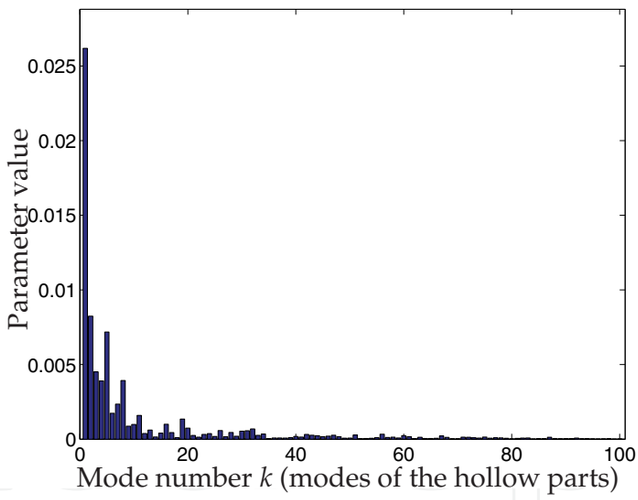

Fig. 16. Values of parameter $\left|\lambda \tilde{G}^k_{H2}\right|$ as a function of k – 50 Hz

3.2.2.3 Path through the hollow parts and the plates

For the vibrational path through the hollow parts and the plates, three modal parameters need to be analyzed. Figures 19 and 20 show the values of modal parameters $\tilde{G}^k_{P11}$ and $\tilde{G}^k_{P13}$ as a function of mode number k for an excitation frequency of 50 Hz. It should be noted that $\tilde{G}^k_{P14} = \tilde{G}^k_{H2}$, as plotted in figure 16. Figures 21 and 22 provide the values of modal parameters $\tilde{G}^k_{P11}$ and $\tilde{G}^k_{P13}$ as a function of mode number k for an excitation frequency of 300 Hz.

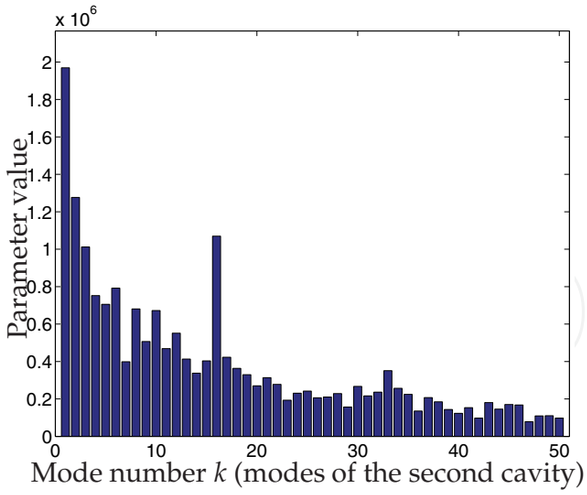

Fig. 17. Values of parameter $\left|\lambda \tilde{G}_{H1}^{k}\right|$ as a function of k – 300 Hz

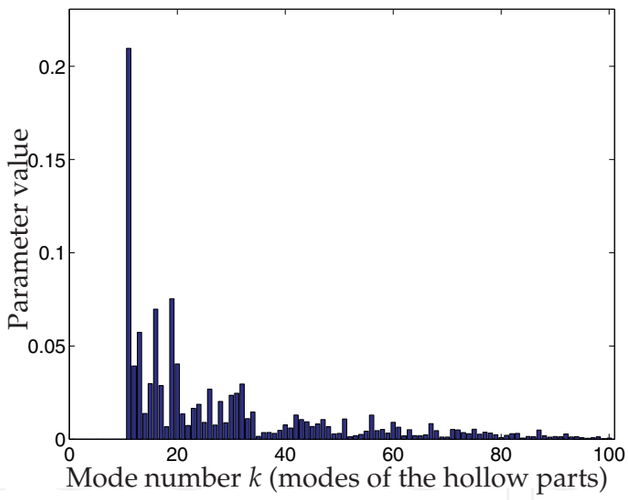

Fig. 18. Values of parameter $\left|\lambda \tilde{G}_{H2}^{k}\right|$ as a function of k – 300 Hz

As reflected in Figures 19 and 20, many modes are strong. Just as in the previous section, it is then possible to optimize the structure using criterion $C_{P14} = C_{H2}^{k}$, so as to minimize the transmission of vibrations through two different paths. It is also possible to minimize criterion C_{P11}, which is greater than C_{P13}.

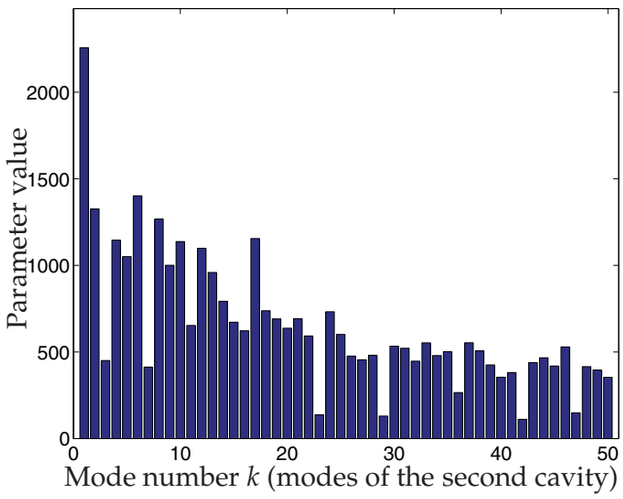

Fig. 19. Values of parameter $\left|\lambda \tilde{G}^{k}_{P11}\right|$ as a function of k – 50 Hz

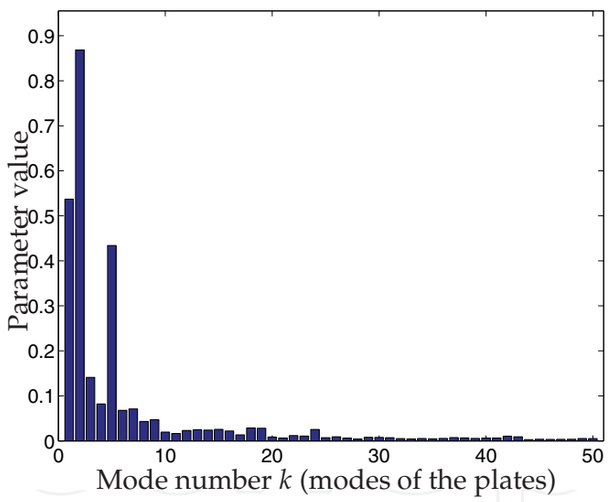

Fig. 20. Values of parameter $\left|\lambda \tilde{G}^{k}_{P13}\right|$ as a function of k – 50 Hz

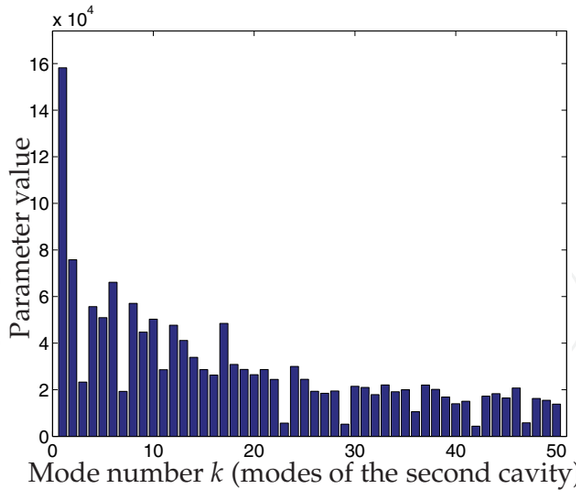

Fig. 21. Values of parameter $\left|\lambda \tilde{G}_{P11}^{k}\right|$ as a function of k – 300 Hz

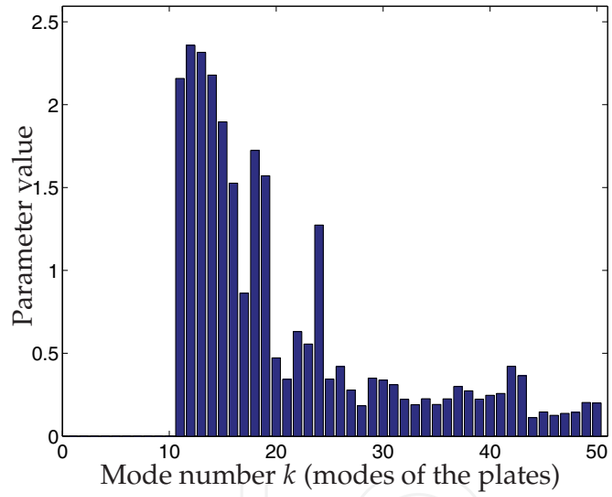

Fig. 22. Values of parameter $\left|\lambda \tilde{G}_{P13}^{k}\right|$ as a function of k – 300 Hz

4. Conclusion

In this chapter, several criteria, corresponding to different vibrational propagation paths, have been proposed. These criteria are based on modal motion equations, which allow for working with small-sized matrices. Consequently, calculation-related costs are not prohibitive during the optimization process, which is an important consideration whenever objective functions have to be evaluated many times. Moreover, a modal overview of the phenomena serves to illustrate the relative influence of each mode on noise propagation, in addition to indicating which part of the system exerts the strongest influence on noise generation inside the structure.

5. References

Besset, S. & Jézéquel, L. (2008a). Dynamic substructuring based on a double modal analysis, *J. Vib. Acoust* 130(1).

Besset, S. & Jezequel, L. (2008b). A modal analysis method to study fluid-structure coupling in hollow parts of a structure, *Journal of Computational Acoustics* 16(02): 257.

Besset, S. & Jézéquel, L. (2008c). Modal criteria for optimization of the acoustical behaviour of a vibroacoustic system based on a systemic approach, *International Journal for Numerical Methods in Engineering* 73: 1347–1373.

Besset, S. & Jézéquel, L. (2008d). Vibroacoustical analysis based on a multimodal strategy: Triple modal synthesis, *J. Vib. Acoust* 130(3).

Craig, R. R. & Bampton, M. C. C. (1968). Coupling of substructures for dynamic analysis, *AIAA Journal* 6: 1313–1321.

Farhat, C. & Géradin, M. (1998). On the general solution by a direct method on a large-scale singular system of linear equations: Application to the analysis of floating structures, *International journal for numerical methods in engineering* 41: 675–696.

Goldman, R. L. (1968). Vibration analysis by dynamic partitioning, *AIAA Journal* 7: 1152–1154.

Hou, S. N. (1969). Review of modal synthesis techniques and a new approach, *Shock and vibration bulletin* 40: 25–30.

Hurty, W. C. (1965). Dynamic analysis of structural systems using component modes, *AIAA Journal* 3: 678–685.

Morand, H. J. & Ohayon, R. (1995). *Fluid Structure Interaction*, Wiley & Sons.

Ohayon, R. (2001). Reduced symetric models for modal analysis of internal structural-acoustic and hydroelastic-sloshing systems, *Computer Methods in Applied Mechanics and Engineering* 190: 3009–3019.

Ohayon, R. (2003). Reduced models for fluid-structure interaction problems, *International Journal for Numerical Methods in Engineering* 60: 139–152.

Sandberg, G. E., Hansson, P.-A. & Gustavsson, M. (2001). Domain decomposition in acoustic and structure-acoustic analysis, *Computer Methods in Applied Mechanics and Engineering* 190: 2979–2988.

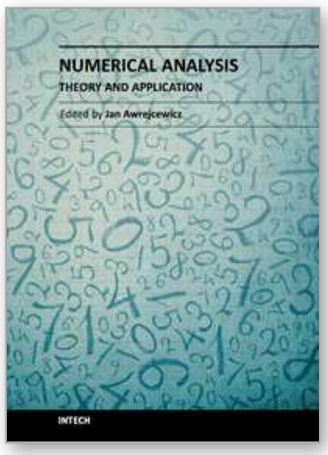

Numerical Analysis - Theory and Application

Edited by Prof. Jan Awrejcewicz

ISBN 978-953-307-389-7
Hard cover, 626 pages
Publisher InTech
Published online 09, September, 2011
Published in print edition September, 2011

Numerical Analysis â€“ Theory and Application is an edited book divided into two parts: Part I devoted to Theory, and Part II dealing with Application. The presented book is focused on introducing theoretical approaches of numerical analysis as well as applications of various numerical methods to either study or solving numerous theoretical and engineering problems. Since a large number of pure theoretical research is proposed as well as a large amount of applications oriented numerical simulation results are given, the book can be useful for both theoretical and applied research aimed on numerical simulations. In addition, in many cases the presented approaches can be applied directly either by theoreticians or engineers.

How to reference

In order to correctly reference this scholarly work, feel free to copy and paste the following:

Sébastien Besset and Louis Jézéquel (2011). Optimization of the Dynamic Behaviour of Complex Structures Based on a Multimodal Strategy, Numerical Analysis - Theory and Application, Prof. Jan Awrejcewicz (Ed.), ISBN: 978-953-307-389-7, InTech, Available from: http://www.intechopen.com/books/numerical-analysis-theory-and-application/optimization-of-the-dynamic-behaviour-of-complex-structures-based-on-a-multimodal-strategy

INTECH
open science | open minds

InTech Europe
University Campus STeP Ri
Slavka Krautzeka 83/A
51000 Rijeka, Croatia
Phone: +385 (51) 770 447
Fax: +385 (51) 686 166
www.intechopen.com

InTech China
Unit 405, Office Block, Hotel Equatorial Shanghai
No.65, Yan An Road (West), Shanghai, 200040, China
中国上海市延安西路65号上海国际贵都大饭店办公楼405单元
Phone: +86-21-62489820
Fax: +86-21-62489821

IntechOpen